https://journal.unnes.ac.id/nju/index.php/sainteknol

Voltammetric Analysis of Pb2+ Ion on Gold Nanoparticles-Modified ZnO Electrode

Rahmi Fauziah, Cepi Kurniawan

Universitas Negeri Semarang, Indonesia

Abstrak

Waste such as heavy metal is a very dangerous toxic material, the heavy metal that is often used is lead (Pb). In this study, heavy metal detection was carried out with the material used, namely ZnO because it has high sensitivity in heavy metal detection. ZnO will be modified with gold nanoparticles (AuNP). AuNP has been used for surface decoration of oxides to obtain high sensor performance which is 6.5 times faster than without the addition of Au. Research has been carried out on the Voltammetric Analysis of Pb^{2+} Ion on Gold Nanoparticles-Modified ZnO Electrode. This study aims to determine the nature and characteristics of the ZnO/AuNP compound deposited on the SPCE electrode and to determine the selectivity and sensitivity of the ZnO/AuNP electrodeposition on the SPCE electrode to identify heavy metals. FTIR characterization showed that there was a Zn-O bond in the synthesized compound. SEM characterization showed hexagonal morphology. The PSA results showed the size of the AuNP was 115.7 nm. The test results of the ZnO/AuNP5%/SPCE electrode sensor have a LoD value of 2.88 ppm and a LoQ of 9.60 ppm, a sensitivity of 0.077 $\mu A\ \mu g^{-1}$ L., and R^2 = 0.96862.

Kata kunci : Zinc Oxide, Pb, Electrodeposition, Anodic Stripping Voltammetry

Introduction

Heavy elements such as mercury, lead, cadmium and cobalt are an important group of pollutants that have been selected as the target for many stripping electoanalytical sensing methodologies at trace and ultratrace levels [1]. Because of the increased industrial use of the metals and their serious environmental impact, the development of new sensitive methods for quantifying trace amounts of these metals is required and challenged. These metal ions frequently coexist in many environmental samples with potential danger to aquatic life, especially at high levels. In recent years, the determination of potentially toxic metal ions in environmental samples has been a common concern, and there is growing need for simultaneous determination of toxic metals.

Lead (Pb) is toxic, according to the Regulation of the Minister of the Environment No. 82 of 2001 concerning the limit on the value of lead content for drinking water is 0.03 mg/L. Cases of heavy metal pollution such as lead (Pb) from industrial waste have resulted in decreased quality of rivers [2]. Based on regulations regarding the maximum concentration of heavy metals, sensors are needed that can detect the presence of heavy metals such as Pb even in small quantities and concentrations. The sensor made is expected to have good sensitivity and selectivity, fast, easy method and can detect below the maximum allowed heavy metal levels.

Analytical methods to measure heavy metal levels have been carried out such as inductively coupled plasma optical emission spectroscopy (ICP-OES), atomic fluorence spectroscopy [3], atomic absorption spectroscopy [4], and atomic flame adsorption spectrometry (FAAS), but this technique is not yet extensively used in underdeveloped countries due to their high implementation and maintenance costs. The electrochemical method is one of the most potential methods for detecting hazardous pollutants, because

this method can analyze quickly, instrumentation is easy, costs are low, and has high sensitivity [5]. The redox properties of active heavy metals make them suitable for detection by electrochemistry. The voltammetry technique has good sensitivity and selectivity in heavy metal detection [6].

ZnO has high sensitivity in various contamination variations such as heavy metals in environmental pollution and shows good adsorption ability on harmful metals [7]. AuNP compounds are reported to improve the properties of a material by acting as an electron transfer mediator and have flexibility in surface modification [8]. The the precious metal Au has been used for surface decoration of oxides to obtain high sensor performance, which is 6.5 times faster than without the addition of Au [9]. In this study, considering the efficiency of the use of modified ZnO semiconductors with AuNP deposited on carbon electrodes, a Pb heavy metal sensor will be developed using an electrochemical method.

Materials potassium ferricyanide ($K_3[Fe(CN)_6]$, potassium chloride (KCl), gold nanoparticles (AuNP, 30%), lead ion standard solution (100 $mg.L^{-1}$), $Zn(NO_3)_2$ (Merck), Zinc acetate ($Zn(OAc)_2$), hexamethylenetetramine ($C_6H_{12}N_4$, HMT), sodium hydroxide (NaOH, Merck), $Pb(NO_3)_2$ (Merck), $Cd(CH_3CO_2)_2$ (Merck), ethanol (Merck) SPCE electrodes and distilled water.

Methods

Synthesis of ZnO and ZnO/Au nanoparticles Synthesis of ZnO/AuNP using a sonochemical reaction between $Zn(NO_3)_2$ (1.2 M), HMT (1.2 M), NaOH (0.6 M) and variations of AuNP (5%, 3%, 1%). 30 mL of the solution was prepared and ultrasonically for 60 minutes at 60°C. Then allowed to separate, the precipitate was removed with aquabidest and ethanol, centrifuged for 5 minutes. The precipitate was obtained in an oven at 120°C for 24 hours [10]. ZnO powder was calcined in a furnace at 400°C for 60 minutes [11].

Electrochemical deposition of ZnO The SPCE electrode was put into a 50 mM $Zn(OAc)_2$ solution with 0.1 M KCl electrolyte which had been aerated with nitrogen for 10 minutes. Then it was allowed to stand for 10 minutes at a potential of 0. Next, electrodeposition was carried out at a potential of -1.5 V for 10 minutes at a temperature of 70°C. The SPCE was then rinsed with aquabidest and ethanol, then dried at room temperature [12].

Cyclic voltammetry of Pb Potentiostats were carried out to characterize various electrodes modified in 1.0 mM $K_3[Fe(CN)_6]$ solution containing 0.1 $mol.L^{-1}$ KCl. ZnO/AuNP/SPCE which has been modified in 0.1 M KCl containing various concentrations of $Pb(NO_3)_2$ solution, namely 100, 50, 20, 15, 10, 5, 1, 0.5, 0.3, and 0.1 ppm with a potential range of -0.4 V to +0.3V at a scan rate variation of 0.5 V/s and a sample rate of 100 Hz [6].

Anodic stripping voltammetry of Pb Anodic Stripping Voltammetry (ASV) method was carried out to characterize SPCE, ZnO/SPCE, and ZnO/AuNP/SPCE electrodes in Pb^{2+} 100 ppm solution which was diluted for each concentration 0; 0.1; 0.3; 0.5; 1; 5; 10 and 15 ppm with 0.1 M KCl solvent. 10 mL of Pb solution was measured in three stages. The first stage is the Preconcentration Step (Deposition) with E = -800 mV (potential when H_2 gas is formed in the SPCE), t = 30 s. The second stage is Aging (Equilibration) with t = 5 s. Then the third stage is Anodic Dissolution Step with a potential scan of -1500 to -100 mV using a Rodeostat.

Characterizations The morphologies were observed by scanning electron microscopy (SEM) on a Jeol Jsm 6510 La, synthesis results ZnO and ZnO/AuNP5% were examined by means of fourier transform infrared spectroscopy (FTIR) analysis, X-Ray diffraction (XRD) data were recorded on a XRD shimadzu 7000, AuNP solutions and the filtrate were characterized by UV-Vis spectroscopy, Particle size analysis gold nanoparticle using the Particle Size Analyzer (PSA), electrochemistry measurements were performed with a wheestat.

Results and Discussion

Synthesis of ZnO and ZnO/Au nanoparticles The synthesis of ZnO using the sonication method was successfully carried out based on the product formed according to the reaction reported [13].

$$Zn(NO_3)_{2\,(aq)} + C_6H_{12}N_{4\,(aq)} \rightarrow [Zn(CH_2)_6N_4)]^2 + 2NO_3^- \quad (1)$$

$$C_6H_{12}N_{4\,(aq)} + 4H_2O \rightarrow C_6H_{12}N_4H_4^+ + 4OH^- \quad (2)$$

Hexamethylenetetraamine Zinc (II) in water increasing OH^- population and this increase results in the formation of an intermediate growth unit $Zn(OH)_4^{2-}$.

$[Zn(CH_2)_6N_4)]^{2+}{}_{(aq)} + + 4OH^- \rightarrow Zn(OH)_4^{2-} + C_6H_{12}N_4$ (3)

$Zn(OH)_4^{2-} \rightarrow Zn(OH)_2 + 2OH^-$ (4)

In this step, $Zn(OH)_4^{2-}$ was kept in the air oven at 120°C and calcined at 400°C so that it was reduced easily melted and formed a ZnO structure.

$Zn(OH)_{2(s)} \rightarrow ZnO_{(s)} + H_2O$ (5)

FTIR Spectra The FTIR spectra were recorded in the spectral range of 400-4000 cm^{-1}. Figure 1 shows the highest peaks of ZnO powder that can be observed at 3435.73 cm^{-1}, 1637.61 cm^{-1}, 1386.33 cm^{-1}, 891 cm^{-1}, and 477.49 cm^{-1}. The wide peak at 3435.73 cm^{-1} indicates the presence of stretching OH bonds which are water molecules from the ZnO surface [14], a small peak at 891 cm^{-1} indicates a nitrate (NO_3^-) group [7]. The peak of 1637.61 cm^{-1} occurred due to the asymmetric and symmetrical stretching of the carbon attached to the ZnO particles during the synthesis [15]. The peak of 1386.33 cm^{-1} shows C-N vibrations related to vibrations of the nitrate anion in the interlayer space [16]. The sharp peak at 477.49 cm^{-1} is associated with vibrating ZnO phonons (light waves in the crystal) and indicates a stretching of the Zn-O bond [7], these results indicate the successful production of ZnO particles. Figure 1 shows the FTIR spectra of ZnO/AuNP5% with a peak width of 3435.75 cm^{-1}, which is the movement characteristic of O-H stretching [17], after adding AuNP as much as 5% the width of the peak of O-H stretching decreases. The strong peak at 1637.75 cm^{-1} indicates vibrations from O-H bending. The absorption peak of ZnO vibrations can be observed at 477.75 cm^{-1}.

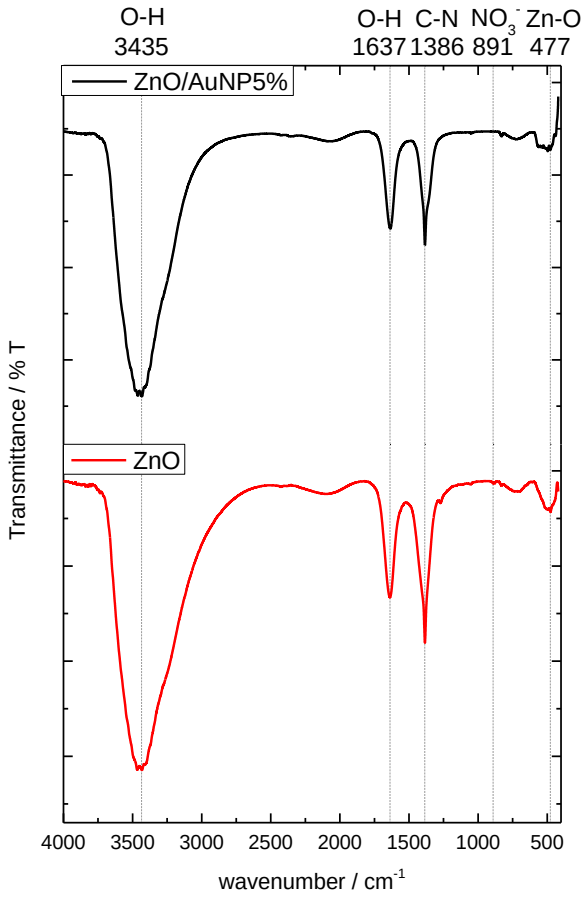

Figure 1. FTIR of ZnO and ZnO/AuNP5%

X-Ray diffraction Characterization using XRD aims to determine the crystal structure of ZnO and

ZnO/AuNP. In Figure 2 the diffraction pattern from the XRD ZnO characterization results shows a sharp peak at 2θ 31.98°; 34.71°; and 36.28°. The angle shows the typical peak indexing the crystal structure of ZnO. Peaks due to impurities were not observed thus confirming that ZnO production was successfully formed [10]. The indication of the shape of ZnO is the hexagonal wurtzite structure (JCPDS 36-1451) [18]. Figure 2 shows the results of the porous ZnO/AuNP5% after being calcined at a temperature of 300°C. ZnO peak at 32.1°; 34.6°; and 36.5° were seen more clearly after calcination [11]. Minor peaks of 43.02 and 44.58 indicate AuNP [19], due to the small AuNP concentration of 5% and large dispersion in the ZnO volume, so these peaks tend to be invisible [20].

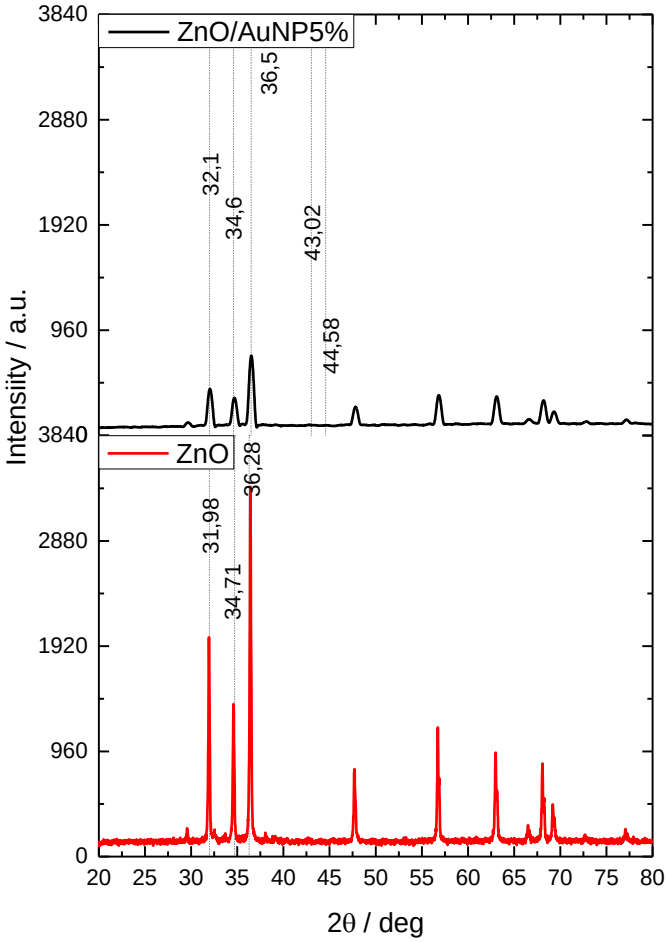

Figure 2. XRD results of ZnO and ZnO/AuNP5%

Scanning electron microscopy Scanning Electron Microscopy (SEM) method was used to analyze the surface morphology and structure of ZnO and ZnO/AuNP. In Figure 3 (a) ZnO powder is magnified 5000x. The formation of ZnO crystals looks like a hexagonal plate on the surface but it is not homogeneous, not clearly visible, and more random [21]. While in Figure 3 (b) shows the results of SEM characterization of ZnO/AuNP there is a significant change in terms of surface morphology on ZnO looks clearer hexagonal shape with a more perfect shape, but the shape that looks still not homogeneous with different lengths and morphology of AuNP has not been seen to coat the surface because the amount is very small compared to ZnO. AuNPs are triangular in shape with a large surface area with a diameter range of 200 nm at high resolution and spherical at 50 nm [14].

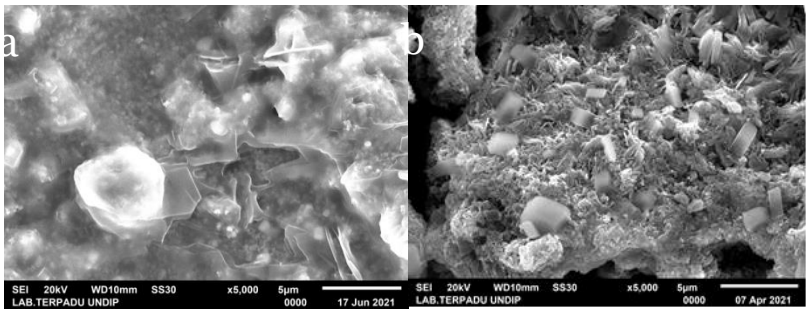

Figure 3. SEM image of (a) ZnO, (b) ZnO/AuNP5%

UV-Vis spectroscopy Figure 4(a) shows the results of the UV-Vis spectra of the standard AuNP solution. The measurements made showed that Au nanoparticles had been formed. There is one absorbance peak resulting from variations in different AuNP concentrations. The peak is at a wavelength of 524 nm [17]. The absorbance peak was higher with increasing AuNP concentration. Figure 4(b) is a comparison between the filtrate sample resulting from the synthesis of ZnO/AuNP with a standard solution of AuNP with variations in concentration, the UV results from the filtrate did not show any AuNP peak so it can be concluded that the AuNP solution had reacted with the residue of ZnO.

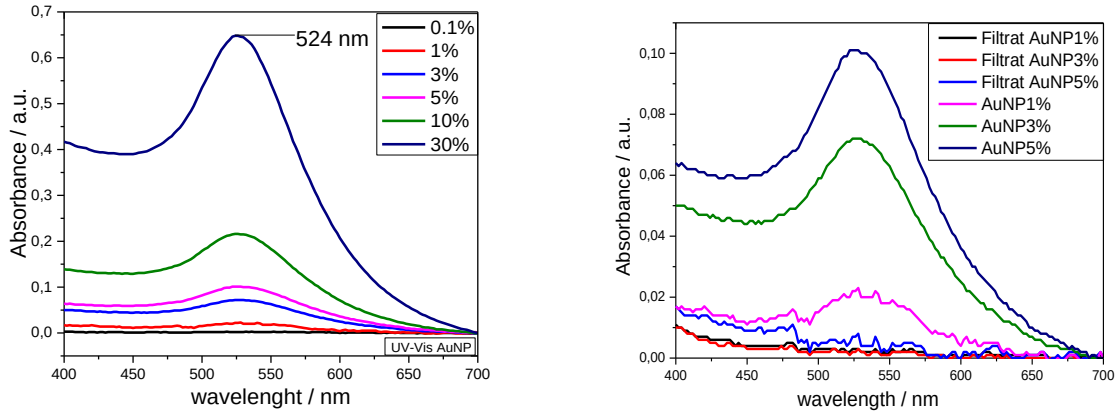

Figure 4. (a) UV-Vis absorption spectra of AuNP solution in different concentrations, (b) UV-Vis absorption spectra comparison between sample filtrate and AuNP standard solution

Particle size analyzer Particle size analysis using the Particle Size Analyzer (PSA) instrument aims to determine the particle size distribution and uniformity of Au nanoparticles at an angle of 173, the sample holder temperature is 25°C, and the shape of the distribution is polydispersion. PSA characterization results are presented in Table 1.

Table 1. Size distribution of AuNP

Calculation Results				
Peak No.	S.P Area Ratio	Mean	S.D.	Mode
1	1.00	212.8 nm	270.7 nm	68.6 nm
2	---	--- nm	--- nm	--- nm
3	---	--- nm	--- nm	--- nm
Total	1.00	212.8 nm	270.7 nm	68.6 nm
Cumulant Operations				
Z-Average				115.7 nm
PI				0.409

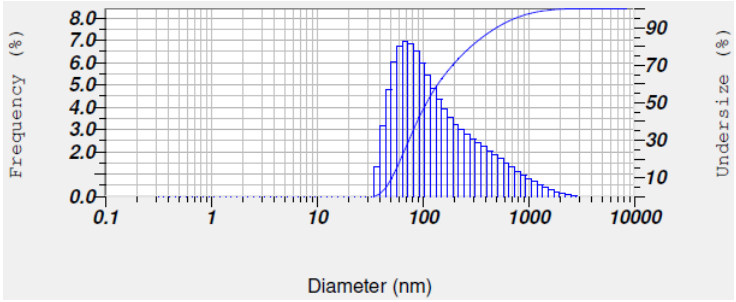

Figure 5. Calculation results PSA of AuNP

Table 1 shows that Au nanoparticles characterized using PSA have a particle size of 115.7 nm and PI (Polydispersity Index) value of 0.409 which indicates a heterogeneous particle size. However, measurements with PSA are still above 100 nm, where the size is said to be nanometers if the size is in the 0-100 nm range [22].

Cyclic voltammetry Reduction oxide reaction ($K_3[Fe(CN)_6]$) was carried out to determine the success of electrode modification by ZnO. The SPCE is a conductive electrode and allows a redox reaction ($K_3[Fe(CN)_6]$) to take place, with an oxidation-reduction peak marked on the voltammogram as shown in Figure 6. Observed in Figure 6a SPCE voltammogram of anodic potential (EA = -6 mV) and cathodic potential (EK = 243 mV) in other words reduction potential ($K_3[Fe(CN)_6]$) (E1/2 = 118.5 mV) with a current of 19.48 µA, this value indicates the SPCE is in a quasi-reversible system because the anodic peak is at a negative potential, while the cathodic peak is at a positive potential. In Figure 6b after modified ZnO/SPCE the current becomes smaller by 1.97 µA which indicates that the SPCE has been covered by ZnO so that no redox reactions occur, anodic potential (EA = 57 mV) and cathodic potential (EK = 183 mV) with in other words reduction potential ($K_3[Fe(CN)_6]$) (E1/2 = 120 mV)). In Figure 6c after the SPCE is modified with ZnO/AuNP the current becomes larger, namely 25.19 µA with anodic potential (EA = 48 mV) and cathodic potential (EK = 219 mV) in other words reduction potential ($K_3[Fe(CN)_6]$) (E1/2 = 133.5 mV). This is because the evenly distributed AuNP will have a large surface area, and excellent electrical conductivity so that it can capture electrons in redox reactions [23].

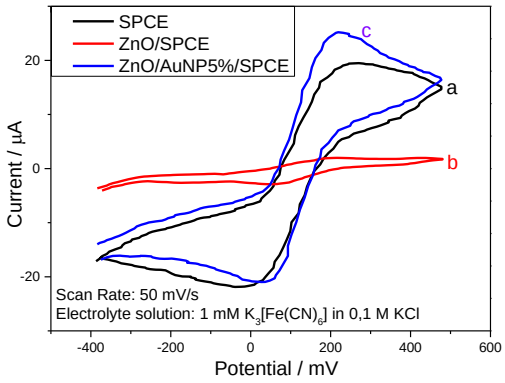

Figure 6. CV characterization of SPCE, ZnO/SPCE, ZnO/AuNP5%/SPCE in $K_3[Fe(CN)_6]$ redox probe

In Figure 7 Pb detection with concentrations of 0.1 - 100 ppm. From the cyclic voltammetry curve performed, it can be seen that the SPCE electrode, ZnO/SPCE and ZnO/AuNP5%/SPCE was successfully carried out to detect Pb but the results obtained were not good as indicated by the variation of the given Pb concentration that did not show a constant change in the oxidation peak. The voltammogram results from the SPCE electrode did not have a tendency at a certain potential and some curves almost overlapped, at the ZnO/SPCE electrode the oxidation peak was not clearly visible at high concentrations and there was

asymmetry between the upper (oxidation) and lower (reduction) components which proved that the process which occurs is irreversible, while at the ZnO/AuNP/SPCE electrode the asymmetry between the oxidation and reduction peaks is less clear. The peak intensity is much lower than ZnO/SPCE, this may indicate that the strength between the lead ion and the ZnO surface is weaker and no proportional ratio of the observed concentrations [24]. From Figure 7 it can be seen that the lower the Pb concentration, the higher the oxidation peak and the higher the Pb concentration the lower the current. This indicates that the Pb sensor with the cyclic voltammetry method using ZnO/AuNP/SPCE electrodes is more sensitive at low concentrations, but has not been able to identify Pb properly when tested with variations in Pb concentrations. This method can detect qualitatively and cannot quantitatively, this is because the AuNP concentration is not homogeneous and cannot confirm the presence of AuNP on the ZnO surface, so AuNP is less able to interact with Pb analytes.

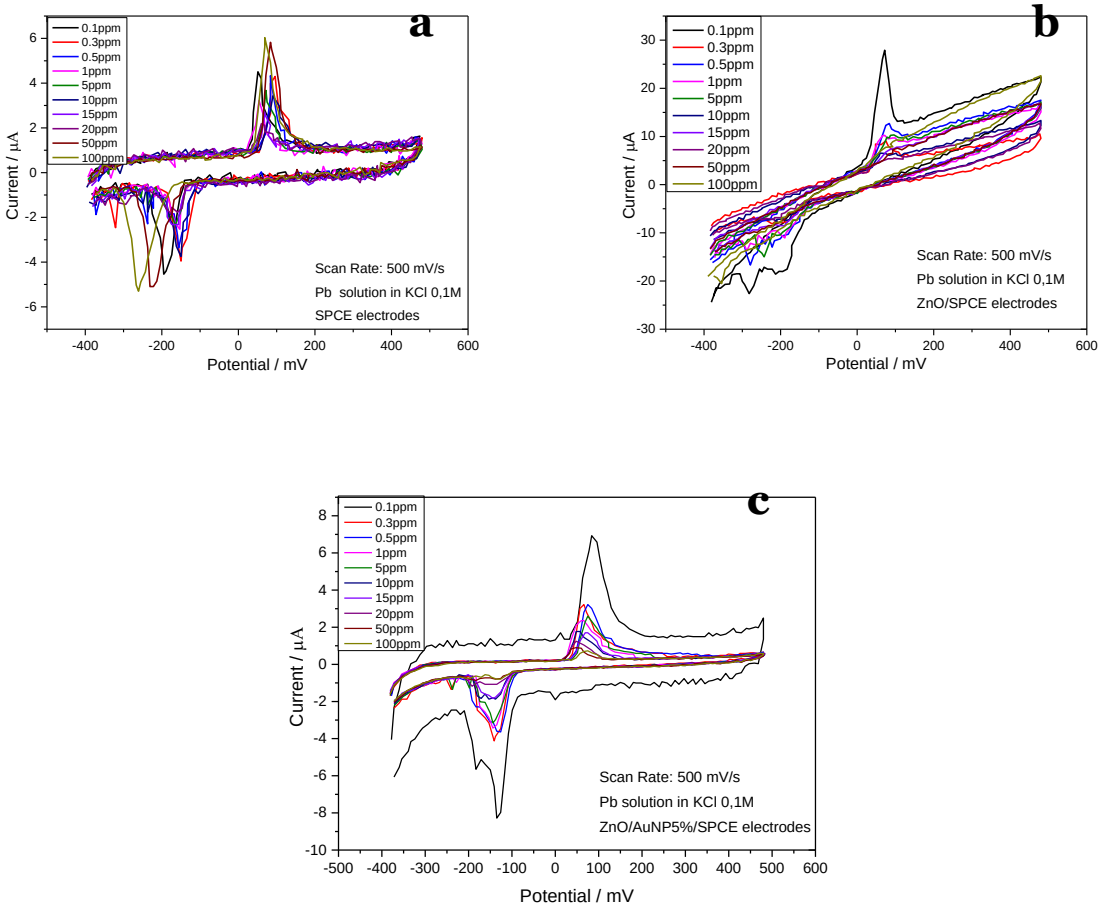

Figure 7. Cyclic voltammogram of (a) SPCE, (b) ZnO/SPCE, (c) ZnO/AuNP5%/SPCE for detection Pb^{2+} at 0,1 – 100 ppm in KCl 0,1 M

Anodic stripping voltammetry In Figure 8 the ASV voltammogram shows a peak of Zn at a potential of -1208 V with a higher current with the variation of AuNP. Zn loses 2 electrons so that the oxidation reaction of $Zn \rightarrow Zn^{2+} + 2e^-$ occurs. When electrodeposition was carried out at -800 mV from the ZnO/SPCE electrode and with AuNP modification, ZnO released oxygen indicating a reduction reaction.

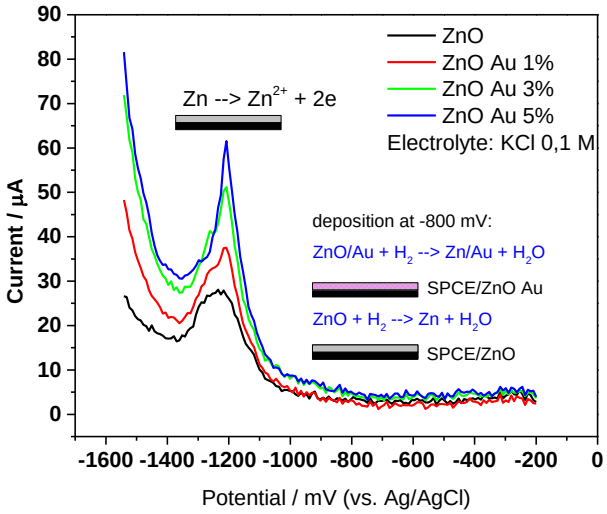

Figure 8. Anodic stripping voltammograms of ZnO/SPCE (black line), ZnO/AuNP1%/SPCE (red line), ZnO/AuNP3%/SPCE (green line), and ZnO/AuNP5%/SPCE (blue line) for detection Pb^{2+} at 0 ppm in KCl 0,1 M

In Figure 9, a comparison of electrode modifications in 15 ppm Pb solution shows a reduction reaction from Pb which accepts 2 electrons to Pb^{2+} in the potential range of -400 mV to -500 mV. This indicates that the modified electrode can detect Pb ions.

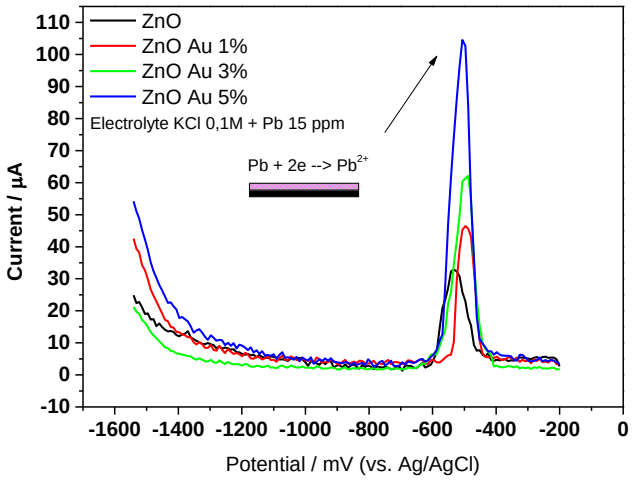

Figure 9. Anodic stripping voltammograms of ZnO/SPCE (black line), ZnO/AuNP1%/SPCE (red line), ZnO/AuNP3%/SPCE (green line), and ZnO/AuNP5%/SPCE (blue line) for detection Pb^{2+} at 15 ppm in KCl 0,1 M

Measuring the selectivity of the ASV method was carried out by testing the current on a solution of Pb, Cd, and a mixed solution of 15 ppm concentration. Based on Figure 10, the ASV voltammogram shows that Pb 15 ppm was detected at a potential of -506 mV with a current of 104.5 µA, and Cd 15 ppm was detected at a potential of -704 mV with a current of 27.86 µA. Then after the solution is mixed with Pb and Cd solutions, it can still be detected, Pb ions are seen at a potential of -497 mV and the current decreases to 58.15 µA, while Cd ions appear at a potential of -713 mV with a current of 26.40 µA in other words almost the same as before mixed. Based on the results obtained indicate that ZnO/AuNP5%/SPCE is selective for Pb and Cd.

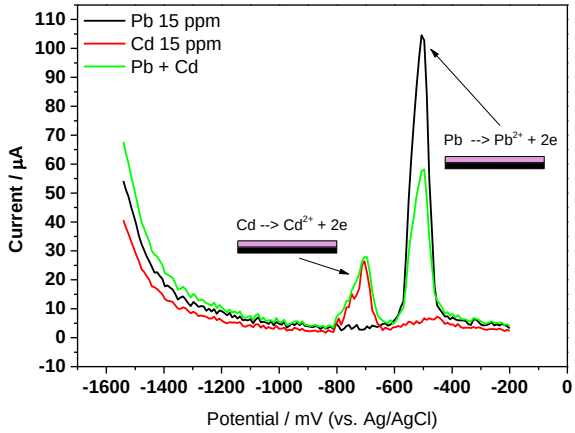

Figure 10. Anodic stripping voltammograms of ZnO/AuNP5%/SPCE for the simultaneous detection of Pb^{2+} and Cd^{2+}

The ASV method is used to obtain a more sensitive peak current. Figure 11 illustrates the voltammogram of heavy metal Pb with various concentrations. The peaks of the detected Pb currents seem to overlap and cannot distinguish the concentrations well, but the ZnO/SPCE electrode successfully detects Pb. Based on the results of plotting the concentration vs current, the sensitivity value and the coefficient of determination (r^2) can be obtained. From the linear graph at Pb concentrations of 0.1 ppm to 15 ppm there is no point on the linear line indicating that ZnO/SPCE does not show a trend in variations in Pb concentration, and the LoD value is 0.55 ppm and LoQ is 1.83 ppm.

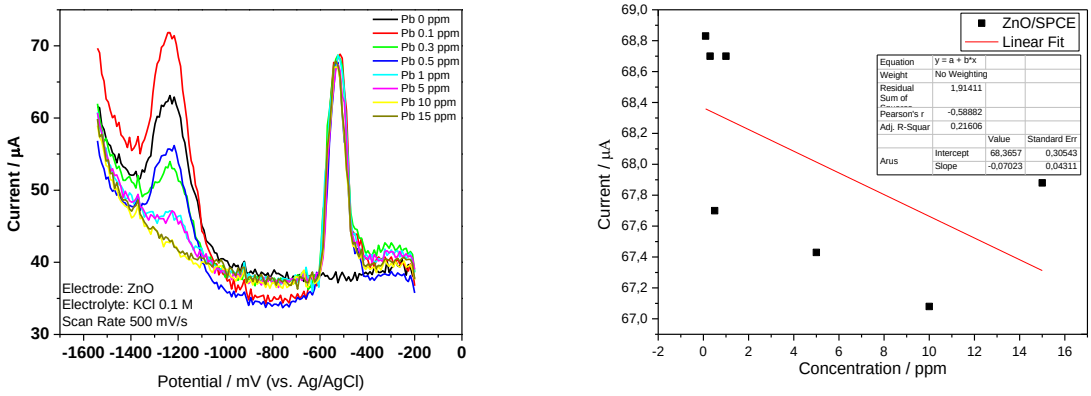

Figure 11. (a) Anodic stripping voltammograms of ZnO/SPCE for detection Pb^{2+} at 0-15ppm (b) Calibration curve for ZnO/SPCE

Figure 12 shows the ASV voltammogram on the ZnO/AuNP1%/SPCE electrode, the ZnO/AuNP1%/SPCE electrodes have not shown a trend as seen from the variation in concentration of the given Pb solution which does not show a good order. From the linear curve of concentration vs current there is no point that is tangent to the linear line and the value of $r^2 = 0.0058$, the value of LoD is 2.16 ppm and the value of LoQ is 7.23 ppm.

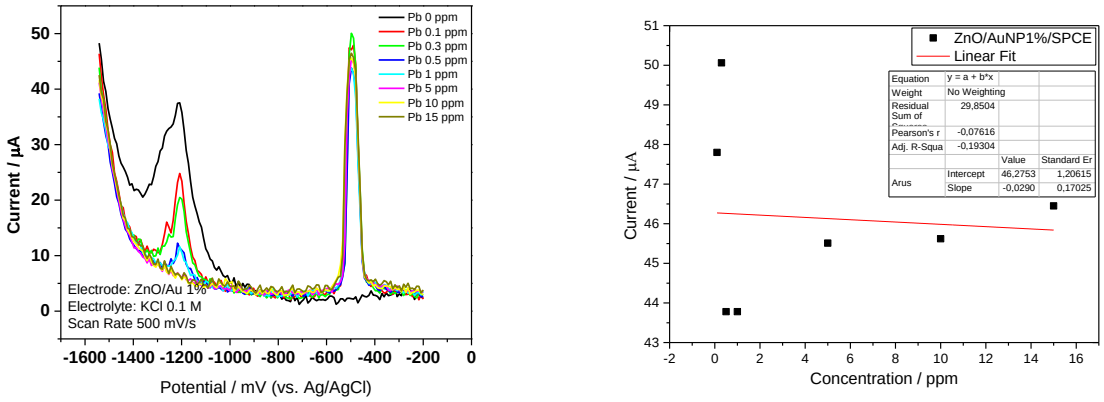

Figure 12. (a) Anodic stripping voltammograms of ZnO/AuNP1%/SPCE for detection Pb^{2+} at 0-15ppm (b) Calibration curve for ZnO/AuNP1%/SPCE

Figure 13 shows the voltammogram of the ZnO/AuNP3%/SPCE electrode, the peak current has shown a good trend where the higher the peak current concentration the higher, but at small concentrations (0.1 ppm and 0.3 ppm) the peak currents still seem to overlap. From the linear curve, the correlation coefficient r^2 is 0.8712 with a LoD value of 2.69 ppm and a LoQ of 8.972 ppm.

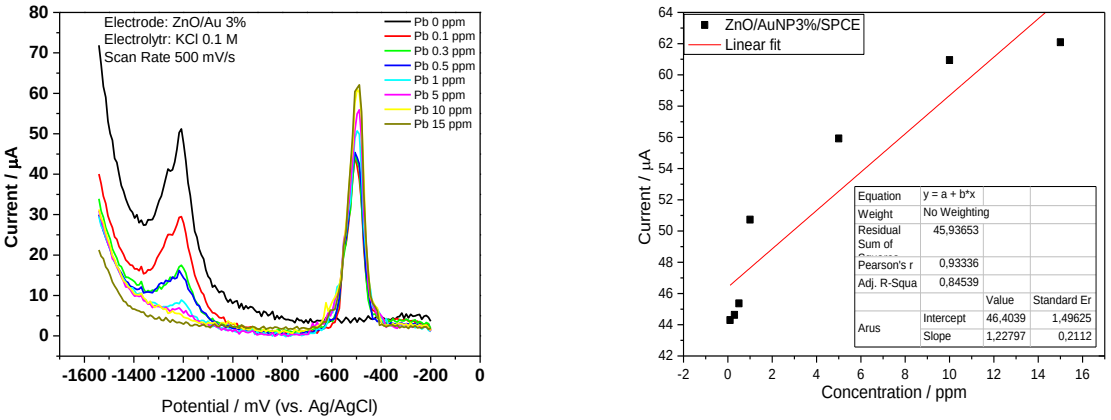

Figure 13. (a) Anodic stripping voltammograms of ZnO/AuNP3%/SPCE for detection Pb^{2+} at 0-15ppm (b) Calibration curve for ZnO/AuNP3%/SPCE

Figure 14 shows the results of the ASV voltammogram on the ZnO/AuNP5%/SPCE electrode, the peak current increases with increasing concentration. From the linear curve shows the r^2 value of 0.973, the correlation coefficient value is higher when compared to other variations, this indicates that the ZnO/AuNP5%/SPCE electrode has given a better trend, the LoD value is 2.88 ppm and the LoQ is 9.60 ppm.

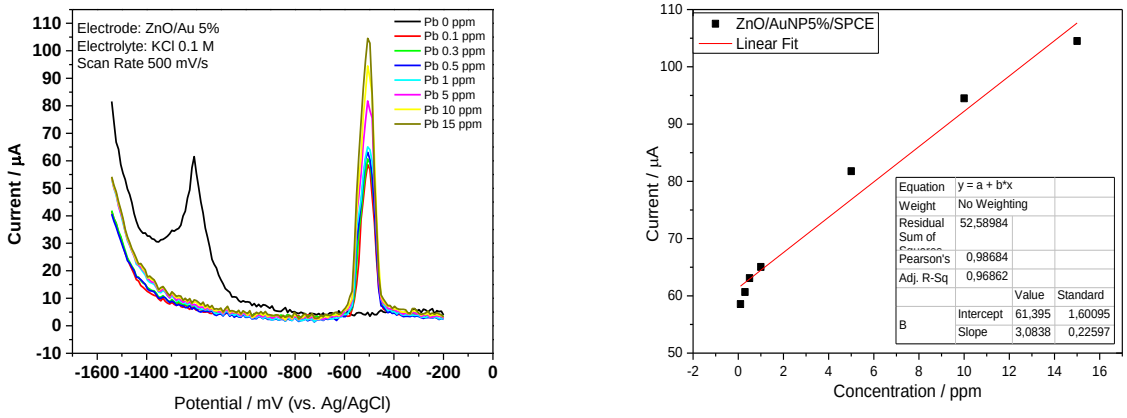

Figure 14. (a) Anodic stripping voltammograms of ZnO/AuNP5%/SPCE for detection Pb^{2+} at 0-15ppm (b) Calibration curve for ZnO/AuNP5%/SPCE

The capability of this study's ZnO/AuNP5%/SPCE sensor was compared with the reported ASV method, as listed in Table 2

Table 2. Comparison of our proposed electrode to the other modified electrodes in the determination of Pb (II)

Electrode	Method	Sensitivity (µA μg^{-1} L)	Reference
ZnO-Gr/SPCE	ASV	0.2803	[25]
Hg-Bi-SWNTs/GCE	ASV	1,15	[1]
Bi-Xerogel/GCE	ASV	1,35	[26]
ZnO/AuNP5%/SPCE	ASV	0.077	*This Work*

The capability of the ZnO/AuNP5%/SPACE sensor for Pb metal in this study was compared with the reported AAS method, as listed in Table 3.

Table 3. Comparison of our method to the other method in the LoD and LoQ

Method	LoD	LoQ	Reference
TS-FF-AAS	6,0 µg/L	20 µg/L	[4]
AAS	0,16 µg/L	0,539 µg/L	[27]
ASV	2.880 µg/L	9.600 µg/L	*This Work*

Based on the comparison with the literature, the ASV method using ZnO/AuNP5%/SPCE electrodes has a smaller sensitivity value and greater LoD and LoQ values, so it can be concluded that this method is good for detecting heavy metal Pb but requires improvements in electrode preparation.

Conclusions

The ZnO compound shows a hexagonal wurtzite structure that is not yet homogeneous. While the structure of ZnO/AuNP shows a clearer hexagonal shape, the morphology of AuNP has not been seen. The peak of the AuNP solution was seen at a wavelength of 524 nm, while the filtrate did not show any AuNP peak which could guarantee that the AuNP solution had reacted with the residue of ZnO. The results of the selectivity test on the ZnO/AuNP5%/SPCE electrode showed the ability to detect heavy metal Pb at a potential of -500 V and Cd at a potential of -700 V. The ZnO/AuNP5%/SPCE sensor has a LoD value of 2.88 ppm and a LoQ of 9.60 ppm, sensitivity 0.077 A g-1 L., and R^2 = 0.96862.

References

[1] R. Ouyang, Z. Zhu, C. E. Tatum, J. Q. Chambers, and Z. Xue, “Simultaneous stripping detection of Zn

(II), Cd (II) and Pb (II) using a bimetallic Hg – Bi / single-walled carbon nanotubes composite electrode," *J. Electroanal. Chem.*, vol. 656, no. 1–2, pp. 78–84, 2011, doi: 10.1016/j.jelechem.2011.01.006.

[2] R. Desriyan, E. Wardhani, and K. Phawmawati, "Identifikasi Pencemaran Logam Berat Timbal (Pb) pada Perairan Sungai Citarum Hulu Segmen Dayeuhkolot sampai Nanjung," *J. Online Inst. Teknol. Nas.*, vol. 3, no. 1, pp. 1–12, 2015.

[3] G. Aragay and A. Merkoc, "Recent Trends in Macro- , Micro- , and Nanomaterial-Based Tools and Strategies for Heavy-Metal Detection," *Chem. Reviws*, vol. 111, no. 5, pp. 3433–3458, 2011, doi: 10.1021/cr100383r.

[4] J. A. Da-col, S. M. A. Domene, and E. R. Pereira-filho, "Fast Determination of Cd , Fe , Pb , and Zn in Food using AAS," *Food Anal. Methods*, vol. 2, no. 2, pp. 110–115, 2009, doi: 10.1007/s12161-008-9041-4.

[5] S. Lee, J. Oh, and D. Kim, "A sensitive electrochemical sensor using an iron oxide / graphene composite for the simultaneous detection of heavy metal ions," *Talanta*, vol. 160, pp. 528–536, 2016, doi: 10.1016/j.talanta.2016.07.034.

[6] G. Bhanjana, N. Dilbaghi, R. Kumar, and S. Kumar, "Electrochimica Acta Zinc Oxide Quantum Dots as Efficient Electron Mediator for Ultrasensitive and Selective Electrochemical Sensing of Mercury," *Electrochim. Acta*, vol. 178, pp. 361–367, 2015, doi: 10.1016/j.electacta.2015.07.113.

[7] A. A. Ibrahim *et al.*, "Talanta Growth and properties of Ag-doped ZnO nanoflowers for highly sensitive phenyl hydrazine chemical sensor application," *Talanta*, vol. 93, pp. 257–263, 2012, doi: 10.1016/j.talanta.2012.02.030.

[8] Y. Cui, Y. Zhao, Y. Tian, W. Zhang, X. Lü, and X. Jiang, "The molecular mechanism of action of bactericidal gold nanoparticles on Escherichia coli," *Biomaterials*, vol. 33, no. 7, pp. 2327–2333, 2012, doi: 10.1016/j.biomaterials.2011.11.057.

[9] Y. V. Kaneti *et al.*, "Hydrothermal synthesis of ternary α-Fe2O3–ZnO–Au nanocomposites with high gas-sensing performance," *Sensors Actuators B. Chem.*, vol. 209, pp. 889–897, 2015, doi: 10.1016/j.snb.2014.12.065.

[10] C. Pholnak, C. Sirisathitkul, S. Danworaphong, and D. J. Harding, "Sonochemical synthesis of zinc oxide nanoparticles using an ultrasonic homogenizer," *Ferroelectrics*, vol. 455, no. 1, pp. 15–20, 2013, doi: 10.1080/00150193.2013.843405.

[11] K. Sowri Babu, A. Ramachandra Reddy, C. Sujatha, K. Venugopal Reddy, and A. N. Mallika, "Synthesis and Optical Characterization of Porous ZnO," *J. Adv. Ceram.*, vol. 2, no. 3, pp. 260–265, 2013, doi: 10.1007/s40145-013-0069-6.

[12] A. H. Ismail, A. H. Abdullah, and Y. Sulaiman, "Physical and Electrochemical Properties of ZnO Films Fabricated from Highly Cathodic Electrodeposition Potentials," *Superlattices Microstruct.*, vol. 103, pp. 171–179, 2017, doi: 10.1016/j.spmi.2017.01.028.

[13] S. Alfarisa, P. L. Toruan, A. Atina, W. S. B. Dwandary, and R. N. Safitri, "Morphological and Structural Studiesof ZnO Micro-Nanorod Structures Synthesized Using a Low-Cost Hydrothermal Method," *Makara J. Sci.*, vol. 22, no. 2, pp. 59–66, 2018, doi: 10.7454/mss.v22i2.8243.

[14] B. S. Bhau, S. Ghosh, S. Puri, B. Borah, D. K. Sarmah, and R. Khan, "Green Synthesis of Gold Nanoparticles from The Leaf Extract of Nepenthes Khasiana and Antimicrobial Assay," *Adv. Mater. Lett.*, vol. 6, no. 1, pp. 55–58, 2015, doi: 10.5185/amlett.2015.5609.

[15] G. S, A. Belay, C. Reddy AR, and B. Z, "Synthesis and Characterizations of Zinc Oxide Nanoparticles for Antibacterial Applications," *J. Nanomed. Nanotechnol.*, vol. S8, no. 004, pp. 1–8, 2017, doi: 10.4172/2157-7439.s8-004.

[16] S. Kumar, M. Ganapathy, S. Sharmila, M. Shankar, M. Vimalan, and I. Vetha Potheher, "ZnO/Ni(OH)2core-shell nanoparticles: Synthesis, optical, electrical and photoacoustic property analysis," *J. Alloys Compd.*, vol. 703, pp. 624–632, 2017, doi: 10.1016/j.jallcom.2017.01.323.

[17] A. Mehrani, D. Dorranian, and E. Solati, "Properties of Au / ZnO Nanocomposite Prepared by Laser Irradiation of the Mixture of Individual," *J. Clust. Sci.*, vol. 26, no. 5, pp. 1743–1754, 2015, doi: 10.1007/s10876-015-0872-z.

[18] A. Saranya, T. Devasena, H. Sivaram, and R. Jayavel, "Role of hexamine in ZnO morphologies at

different growth temperature with potential application in dye sensitized solar cell," *Mater. Sci. Semicond. Process.*, vol. 92, no. February, pp. 108–115, 2019, doi: 10.1016/j.mssp.2018.03.028.

[19] R. Jain, A. Thakur, P. Kumar, and D. Pooja, "Au/ZnO nanocomposites decorated ITO electrodes for voltammetric sensing of selenium in water," *Electrochim. Acta*, vol. 290, pp. 291–302, 2018, doi: 10.1016/j.electacta.2018.09.061.

[20] W. Nawrot, O. Rac-rumijowska, and H. Teterycz, "Improving the sensitivity of the ZnO gas sensor to dimethyl sulfide," *IOP Conf. Ser. Mater. Sci. Eng.*, vol. 104, pp. 1–8, 2016, doi: 10.1088/1757-899X/104/1/012030.

[21] L. Sun *et al.*, "Gold nanoparticles modified ZnO nanorods with improved photocatalytic activity," *J. Colloid Interface Sci.*, vol. 363, no. 1, pp. 175–181, 2011, doi: 10.1016/j.jcis.2011.07.005.

[22] A. Marfina, E. Cahyono, S. Mursiti, and Harjono, "Sintesis Nanopartikel Emas dengan Bioreduktor Minyak Atsiri Kayu Manis (Cinnamomum burmannii)," *Indones. J. Chem. Sci.*, vol. 8, no. 2, pp. 2–8, 2019.

[23] Z. Lu, J. Zhang, W. Dai, X. Lin, J. Ye, and J. Ye, "A Screen-Printed Carbon Electrode Modified with A Bismuth Film and Gold Nanoparticles for Simultaneous Stripping Voltammetric Determination of Zn(II), Pb(II) and Cu(II)," *Microchim. Acta*, vol. 184, no. 12, pp. 4731–4740, 2017, doi: 10.1007/s00604-017-2521-8.

[24] M. Krasovska *et al.*, "ZnO-nanostructure-based electrochemical sensor : Effect of nanostructure morphology on the sensing of heavy metal ions," pp. 2421–2431, 2018, doi: 10.3762/bjnano.9.227.

[25] J. Yukird, P. Kongsittikul, J. Qin, O. Chailapakul, and N. Rodthongkum, "ZnO@graphene nanocomposite modified electrode for sensitive and simultaneous detection of Cd (II) and Pb (II)," *Synth. Met.*, vol. 245, no. July, pp. 251–259, 2018, doi: 10.1016/j.synthmet.2018.09.012.

[26] P. A. Dimovasilis and M. I. Prodromidis, "Analytica Chimica Acta Bismuth-dispersed xerogel-based composite films for trace Pb (II) and Cd (II) voltammetric determination," *Anal. Chim. Acta*, vol. 769, pp. 49–55, 2013, doi: 10.1016/j.aca.2013.01.040.

[27] A. B. Shetata, R. N. Yamani, and I. F. Tahoun, "Validation of a method for quantification of Lead , Chromium , Magnesium , Zinc & Copper in human blood and serum using Atomic Absorption Spectrometry," *J. Phys.*, pp. 1–4, 2018, doi: 10.1088/1742-6596/1065/24/242002.